Stability Analysis on Mixed Convection Nanofluid Flow in a Permeable Porous Medium with Radiation and Internal Heat Generation

Shahirah Abu Bakar[1,*], Norihan Md Arifin[2,3], Ioan Pop[4]

1 Takasago Thermal/Engineering Systems Laboratory, Malaysia-Japan International Institute of Technology, Universiti Teknologi Malaysia, 54100, Kuala Lumpur, Malaysia
2 Institute for Mathematical Research, Universiti Putra Malaysia, 43400, UPM Serdang, Selangor, Malaysia
3 Department of Mathematics & Statistics, Faculty of Science, Universiti Putra Malaysia, 43400, UPM Serdang, Selangor, Malaysia
4 Department of Mathematics, Babes-Bolyai University, R-40084 Cluj-Napoca, Romania

ABSTRACT

We investigated the mixed convection boundary layer flow over a permeable surface embedded in a porous medium, filled with a nanofluid and subjected to thermal radiation, magnetohydrodynamics (MHD) and internal heat generation. The nanofluid consists of water (H_2O) as the base fluid and nanoparticles such as copper (Cu), aluminium oxide (Al_2O_3) and titanium dioxide (TiO_2). The governing system nonlinear partial differential equations is transformed into a set of ordinary differential equations using a similarity transformation, which are then solved numerically for various parameter values. The numerical solutions are obtained using the shooting technique method and bvp4c method, via MAPLE and MATLAB, respectively. Our findings revealed that the velocity distribution decreases with the shrinking parameter, while the presence of nanoparticles enhances the respective profiles. The velocity profiles were also observed to exhibit mixed patterns influenced by magnetic, radiation, and suction parameters. Further, the solutions bifurcated into two branches prior to the shrinking parameter. A stability analysis is performed to determine the stability of the solutions between two branches. We thoroughly discussed the characteristics of the respective solutions and their stability in detail.

Keywords:
Nanofluid; internal heat generation;
porous medium; shrinking sheet; dual
solutions; stability analysis

1. Introduction

A comprehensive understanding of flow and heat transfer through permeable surfaces holds significant potential for various technological and engineering applications, including wire drawing, glass-fiber and paper productions, insulation design, among others. Over the past four decades, extensive research has been conducted to improve the thermal efficiency, leading to energy savings and cost reductions in various manufacturing processes. Among the various methods explored, nanofluids were first introduced by Choi and Eastman [1] in 1995, where they dispersed nanometer-sized particles in a base fluid. Their findings revealed that nanoparticles effectively disrupt nanoscale particles, leading to increased thermal transmittance rate. Subsequently, the implementation of

---

* *Corresponding author*
Email address: shahirah.abubakar@utm.my

nanofluids in industrial cooling, as initiated by Routbort *et al.,* [2] in 2008, showed promise in achieving emission reductions and energy savings. Nanofluids have demonstrated the potential to conserve significant amounts of energy in the U.S. industries, with the electric power sector alone capable of liberating 1.055×10^{15} joule of energy when nanofluids are employed in closed-loop cooling cycles. Additionally, the use of nanofluids has been associated with substantial reductions in emissions of NO, CO_2 and SO_2 [3].

Numerous studies have explored the impact of nanofluids on heat transfer rates in various contexts. For instance, Hosseini *et al.,* [4] analysed nanofluid flow in a microchannel heat sink with a magnetic field, while Maleki *et al.,* [5] investigated nanofluid flow over a porous plate considering slip and radiation. Du *et al.,* [6] experimented with CuO/water nanofluid in a geothermal heat exchanger, observing a remarkable 40% increase in heat transfer rate and a 20% improvement in the heat load-to-pumping power ratio. Further investigations by Saffarian *et al.,* [7] demonstrated that the addition of nanofluids enhances heat transfer rates, with CuO nanofluids showing the highest performance in terms of heat transfer coefficient and Nusselt number. Recent contributions by authors such as Kumar and Sonawane [8], Sheikoleslami [9], Sheikholeslami and Vajravelu [10], Bahmani *et al.,* [11], Nazari *et al.,* [12], and Jung and Park [13] have further advanced our understanding in this field.

Moreover, Routbort *et al.,* [2] started a project in 2008 by employing nanofluids in industrial cooling that would develop emission reductions and energy savings. The application of nanofluids in heating and cooling water has the potential to conserve 1.055×10^{15} joule of energy The analysis of nanofluid in a microchannel heat sink with magnetic field is studied by Hosseini *et al.,* [4], while Maleki et al., [5] explored the study of nanofluid flow over a porous plate with slip and radiation. Du *et al.,* [6] experimented a nanofluid of CuO/water in geothermal heat exchanger, where their study observed an increase in heat transfer rate nearly by 40% and the heat load-to-pumping power ratio improved by 20%. Saffarian *et al.,* [7] later reported in their work that the addition of nanofluids increases the heat transfer rate, where CuO at 4% by the wavy collector shows the highest performance in heat transfer coefficient and Nusselt number. Recently, several authors such as Kumar and Sonawane [8], Sheikholeslami [9], Sheikholeslami and Vajravelu [10], Bahmani *et al.,* [11], Nazari *et al.,* [12] and Jung and Park [13].

Porous media, consisting of solid materials with pore structures filled with fluid, play a crucial role in material sciences. The properties of porous media vary based on the internal organization of the pores. Research on fluid flow through porous media has become increasingly relevant in applications such as nuclear waste disposal, inkjet printing, energy conversion storage, and oil recovery systems. Barnoon and Toghraie [14] investigated the laminar flow of non-Newtonian nanofluids in a porous medium, discovering that nanofluid velocity increases with the thicknesses of the porous layer. Additionally, Hassan *et al.,* [15] observed increased heat transfer rates with the addition of nanoparticles to the fluid, while Ahmad *et al.,* [16] concluded that the porosity of the medium elevates the dimensionless streamwise velocity. Subsequent studies by Hayat *et al.,* [17] explored the influence of variable characteristics in unsteady flow of nanofluids past a porous medium. Recent works by Haq *et al.,* [18], Liu *et al.,* [19], Nazari *et al.,* [20], Shah *et al.,* [21], Siavashi *et al.,* [22], and Habibishandiz and Saghir [23] have further advanced our understanding of nanofluid flow imbedded in a porous medium.

Further, internal heat generation occurs where heat is uniformly generated throughout the material at a constant rate, such as when heat is generated through metals or electrical conductors due to passage of current. Benefits of internal heat generation vary especially in science and technological industries, including chemically reactant systems, nuclear reactors and current carrying conductor. Chamkha and Aly [24] studied a natural convection nanofluid flow over a vertical plate

with heat generation and absorption, where the local skin friction coefficient proves to be improved with heat generation parameter. A previous work of heat generation and absorption on nanofluid flow with convective boundary conditions and was reported by Alsaedi *et al.,* [25], while Mahmoudi *et al.,* [26] explored the nanofluid flow in a cavity with entropy generation, heat generation/absorption and magnetic field. Hosseini *et al.,* [27] investigated the nanofluid flow in a heated porous microchannel with entropy generation and heat generation and additionally, the effects of heat generation and viscous dissipation on Ag/water nanofluid flow past a Riga plate was reported by Mishra and Kumar [28]. Further analysis of internal heat generation in nanofluid flow has been studied successfully by Akinshilo [29], Alzahrani *et al.,* [30], Ali *et al.,* [31], Abdulkadhim *et al.,* [32], Ferdows [33] and Elbashbeshy *et al.,* [34].

On the other hand, mixed convection problem in a porous medium has also been widely studied as reported by Merkin [35], Chamkha [36], *Yasin et al.,* [37], just to name a few. At the same time, an adequate understanding of radiative heat transfer in flow processes is very important in engineering and industry fields. Thermal radiation can be explained as electromagnetic radiation generated by the thermal motion of charged particles in matter. Thermal radiation effects are extremely important in the flow processes involving high temperature because thermal radiation can significantly affect the heat transfer and the temperature distribution in the boundary layer flow of participating fluids when the temperatures are high. To achieve a better control on the rate of cooling, considerable efforts have been made in recent years and among other methods, it has been proposed as it may be advantageous to alter the kinematics flow in such a way as to ensure the solidification at the slower rate. Meanwhile, the concept of magnetohydrodynamics or MHD is that magnetic fields can induce currents in a moving conductive fluid, which in turn creates forces on the fluid and changes the magnetic field itself. Studies on thermal radiation and MHD effects on mixed convection are still limited, but had been successfully reported by several authors such as Chamkha and Ben-Nakhi [38], Aydin and Kaya [39], Shateyi *et al.,* [40], Makinde [41] and others.

The principal aim of this study is to evaluate the MHD mixed convection boundary layer flow past a permeable surface in a porous medium filled with a nanofluid with thermal radiation and internal heat generation effects, while the basic fluid being water. Three types of nanoparticles namely Cu (copper), Al_2O_3 (aluminium) and TiO_2 (titanium) are considered in this research. By applying the similarity transformation technique, we transform the governing PDEs into a system of ODEs. We then employ the shooting method implemented in MAPLE and bvp4c solver in MATLAB to obtain the numerical results. The results are then presented in the form of figures and tables, providing a comprehensive visual representation of the findings. Further, a stability analysis is performed to determine the stability of the dual solutions obtained. Overall, this study aims to contribute to the understanding of the combined effects of mixed convection and internal heat generation on nanofluid flow embedded in a porous medium.

2. Mathematical Modelling

In this study, we consider a steady mixed convection boundary layer flow over a permeable surface, passing a vertical semi-infinite plate embedded in a porous medium filled with a nanofluid. Additionally, the presence of thermal radiation and MHD is accounted for as depicted in Figure 1. Following the model proposed by Tiwari and Das [42], the governing equations for the system are
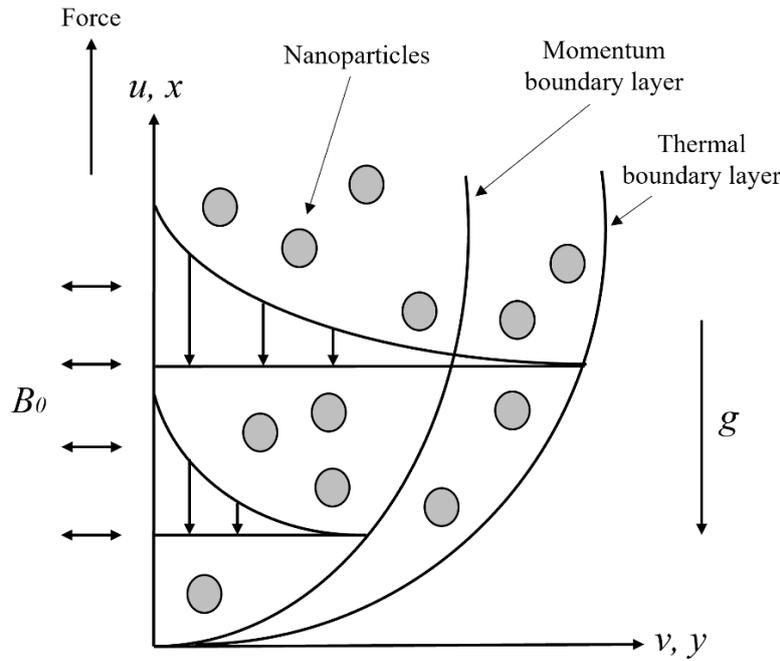
Fig. 1. Physical diagram of the flow model

$$\frac{\partial u}{\partial x} + \frac{\partial v}{\partial y} = 0,$$

(1)

$$\frac{\mu_{nf}}{\mu_f} u = \frac{\mu_{nf}}{\mu_f} U_\infty + \frac{gK\left[\varphi\rho_s\beta_s + (1-\varphi)\rho_f\beta_f\right]}{\mu_f}(T - T_\infty) + \frac{\sigma B_0^2}{\rho_{nf}} u,$$

(2)

$$u\frac{\partial T}{\partial x} + v\frac{\partial T}{\partial y} = \alpha_{nf}\frac{\partial^2 T}{\partial y^2} + \frac{q'''}{(\rho C_p)_{nf}} - \frac{1}{(\rho C_p)_{nf}}\left(\frac{\partial q_r}{\partial y}\right),$$

(3)

$$v = v_w, \; T = T_w(x) \text{ at } y = 0,$$
$$u \to U_\infty, \; T \to T_\infty \text{ as } y \to \infty.$$

(4)

In the above equations, u and v represent the velocity components along the x and y-axes, respectively. The variable g denotes the acceleration due to gravity; K stands for the porous medium permeability, T is nanofluid temperature, and φ represents the nanoparticle volume fraction. Additionally, the properties μ, β, ρ and α are dynamic viscosity, thermal expansion coefficient, fluid density and thermal diffusivity, respective, where the subscripts of f, nf and s refer to the fluid, nanofluid, and solid phases. Another respective variable is B_0, which represents the magnetic field, and q''' denotes the internal heat generation, while q_r is the radiative heat flux. Prior to applying Rosseland's approximation for radiation [43],

we express $q_r = \dfrac{-4\sigma}{3k*}\dfrac{\partial T^4}{\partial y}$

where σ is Stefan Boltzmann constant and $k*$ is mean absorption coefficient.

Considering that the differences in temperature within the flow are sufficiently small, we can express $T^4 \approx 4T_\infty^3 T - 3T_\infty^4$ as a linear function of temperature T using a truncated Taylor series about the free stream temperature T_∞. This approximation allows us to simplify Eq. (3) into

$$u\frac{\partial T}{\partial x} + v\frac{\partial T}{\partial y} = \alpha_{nf}\frac{\partial^2 T}{\partial y^2} + \frac{q'''}{\left(\rho C_p\right)_{nf}} - \frac{16\sigma T_\infty^3}{3k^*\left(\rho C_p\right)_{nf}}\frac{\partial^2 T}{\partial y^2}.$$

(5)

Following Oztop and Abu-Nada [44], the physical properties of nanofluids can be stated as

$$\mu_{nf} = \frac{\mu_f}{\left(1-\varphi\right)^{2.5}}, \quad \alpha_{nf} = \frac{k_{nf}}{\left(\rho C_p\right)_{nf}},$$

$$\left(\rho C_p\right)_{nf} = \left(1-\varphi\right)\left(\rho C_p\right)_f + \varphi\left(\rho C_p\right)_s,$$

$$\frac{k_{nf}}{k_f} = \frac{\left(k_s + 2k_f\right) - 2\varphi\left(k_f - k_s\right)}{\left(k_s + 2k_f\right) + \varphi\left(k_f - k_s\right)},$$

(6)

where ρC_p is capacitance of heat. The respective similarity variables now can be introduced to

$$\psi = \alpha_f\sqrt{Pe_x}f\left(\eta\right), \quad \theta\left(\eta\right) = \frac{T-T_\infty}{T_w-T_\infty}, \quad \eta = \sqrt{\frac{Pe_x}{2}}\frac{y}{x}.$$

(7)

Here, η is similarity variable, Pe_x is local Peclet number for the porous medium, and ψ is stream function which defined by $u = \partial\psi/\partial y$ and $v = -\partial\psi/\partial x$. By substituting Eq. (7) into Eq. (1), (2) and (5), we obtain the following system of ordinary differential equations as:

$$f'\left[\frac{1}{\left(1-\varphi\right)^{2.5}} - M\right] = \frac{1}{\left(1-\varphi\right)^{2.5}} + \left[\left(1-\varphi\right) + \frac{\varphi\rho_s\beta_s}{\rho_f\beta_f}\right]\lambda\theta,$$

(8)

$$\theta''\left[\frac{k_{nf}/k_f}{\left(1-\varphi\right) + \frac{\varphi\rho_s C_{ps}}{\rho_f C_{pf}}} - \frac{4}{3}Rd\right] + f\theta' + \frac{\rho_f}{\rho_{nf}}Q = 0,$$

(9)

prior to the reduced form of boundary conditions at

$$f\left(0\right) = S, \quad \theta\left(0\right) = 1 \text{ at } y = 0,$$
$$f'\left(\eta\right) \to 1, \quad \theta\left(\eta\right) \to 0 \text{ as } \eta \to \infty,$$

(10)

where the respective parameters of *λ, M, Rd, Q* and *S* denote to mixed convection, magnetic, radiation, internal heat generation and suction, which is defined by

$$\lambda = \frac{Ra_x}{Pe_x}, \quad M = \frac{\sigma B_0^2}{\rho_{nf}}, \quad Rd = \frac{4\sigma T_\infty^3}{\alpha_f k * \left(\rho C_p\right)_{nf}}, \quad Q = \frac{q'''}{\left(\rho C_p\right)_f}, \quad S = \frac{-v_w}{U_\infty \alpha_f}.$$

(11)

The representative of λ correspond to an assisting flow or heated plate when $\lambda > 0$, whereas $\lambda < 0$ represents opposing flow/cooled flow, and $\lambda = 0$ is forced convection flow. Prior to the characteristics of porous medium, the combination of Eq. (8) and (9) arises from the extended Darcy law that applied to the two phases, leading to the following expression

$$f''' \left[D_1 - \frac{4}{3} Rd - (1-\varphi)^{2.5} D_1 M + \frac{4}{3} Rd (1-\varphi)^{2.5} M \right] + ff'' \left[1 - (1-\varphi)^{2.5} M \right] + D_2 Q\lambda = 0,$$

(12)

subjected to the simplified boundary conditions at

$$f(0) = S, \quad \frac{1}{(1-\varphi)^{2.5}} f'(0) = \frac{1}{(1-\varphi)^{2.5}} + \left[(1-\varphi) + \frac{\varphi \rho_s \beta_s}{\rho_f \beta_f} \right] \lambda,$$

$$f'(\infty) \rightarrow 1.$$

(13)

Here, $D_1 = \dfrac{k_{nf}/k_f}{(1-\varphi) + \dfrac{\varphi \rho_s C_{ps}}{\rho_f C_{pf}}}$ and $D_2 = \dfrac{\rho_f}{\rho_{nf}} (1-\varphi)^{2.5} \left[(1-\varphi) + \dfrac{\varphi \rho_s \beta_s}{\rho_f \beta_f} \right]$

Another significant physical quantity of practical interest in this study is skin friction coefficient C_f, as it defines the understanding and analysing fluid flow behaviours over surfaces. Skin friction coefficient represents the frictional force per unit area acting on the surface of an object immersed in a fluid flow. Since C_f quantifies the drag or resistance by the surface, hence, understanding the skin friction coefficient is vital in many engineering and scientific contexts. We now introduce C_f in terms of in terms of dimensionless wall shear stress $f''(0)$ as

$$C_f = \frac{\tau_w}{\rho_f U_\infty^2},$$

(14)

where τ_w is the skin friction of the shear stress at the plate surface, which is given by

$$\tau_w = \mu_{nf} \left(\frac{\partial u}{\partial y} \right)_{y=0}.$$

(15)

By substituting Eq. (7) in Eq. (14)-(15), we finally get:

$$\sqrt{2Pe_x} \, C_f = \frac{1}{(1-\varphi)^{2.5}} f''(0).$$

(16)

3. Results and Discussions

The numerical solutions for the governing ordinary differential equations in Eq. (12) are computed using the shooting technique method, while considering the boundary conditions specified in Eq. (13). The results obtained from this analysis facilitate a comprehensive parametric study, exploring the effects of various parameters involved, such as mixed convection parameter λ, nanoparticle volume fraction parameter φ, magnetic parameter M, radiation parameter Rd, and suction parameter S. The study investigates the performance of three types of nanoparticles, namely Cu (copper), Al_2O_3 (aluminium oxide) and TiO_2 (titanium dioxide), in the presence of internal heat generation. For accurate simulations, the physical properties of both fluid and nanoparticles are listed in Table 1.

To assess the reliability of our findings, we compare the values of skin friction coefficient $\frac{1}{(1-\varphi)^{2.5}} f''(0)$ with those reported by Ahmad and Pop [45] in Table 2. Our comparison exhibits excellent agreement, instilling confidence in the accuracy of the numerical results obtained in this study.

Table 1
Physical properties of fluid and selected nanoparticles

Physical Properties	Fluid	Cu	Al_2O_3	TiO_2
C_p (J/kg K)	4179	385	765	686.2
P (kg/m^3)	997.1	8933	3970	4250
k (W/m K)	0.613	400	40	8.9538
$\beta \times 10^{-5}$ (1/K)	21	1.67	0.85	0.9

Table 2
Comparison for values of $\frac{1}{(1-\varphi)^{2.5}} f''(0)$

λ	Present		Ahmad and Pop [45]	
	First Branch of Solution	Second Branch of Solution	First Branch of Solution	Second Branch of Solution
-1.10	0.461049	0.001942	0.46105	0.00194
-1.15	0.449074	0.008658	0.44907	0.00866
-1.20	0.430151	0.022185	0.43015	0.02218
-1.25	0.401524	0.045390	0.40152	0.04539
-1.30	0.356638	0.084871	0.35664	0.08487
-1.35	0.257581	0.178558	0.25758	0.17856

Considering Cu-water and $\varphi = M = Rd = Q = S = 0.0$

In this present study, the values of skin friction coefficient for three types of nanoparticles are shown in detail in Figure 2 where a non-unique solution is observed within the range of $\lambda < 0$. This non-unique solution causes the bifurcation of branches, resulting in two solutions known as the first and second solutions (or first and second branches). The critical value of the solution, denoted as λ_c, corresponds to the peak of this bifurcation. From Figure 2, the skin friction coefficient of Cu-water bifurcates within the range of $-3.61722 < \lambda < 0$, followed by the Al_2O_3-water at $-4.02518 < \lambda < 0$ and TiO_2-water where the range of λ is $-4.01312 < \lambda < 0$. Figure 3 presents a plot of skin friction coefficients of Cu-water against several values of the radiation parameter Rd. As depicted in Figure 2, we observe the occurrence of dual solutions for specific ranges of λ, when Rd is increased. It is noticed that the heat transmittance de-escalates as Rd increases, which can be explained by the

decreasing amount of mean absorption coefficient resulting in less degree of heat transfer rate and this implies that the *Rd* has the effect of expanding the boundary layer separation.

Variation values of mixed convection parameter λ against velocity profiles $f'(\eta)$ is presented in Figure 4 while other parameters are constant. Three types of nanoparticles are considered in the analysis, and it is clearly seen that both solutions decrease when λ increases. This phenomenon is attributed to a significant temperature gradient, which impacts the buoyancy level and directly influences the fluid convection. Initially, buoyancy forces drive the fluid flow by possessing a favourable temperature gradient. However, as the temperature rises, both thickness of the boundary layer and temperature profile decline. Figure 5 then plotted $f'(\eta)$ with the parameter of nanoparticle volume fraction φ, where it is observed that all solutions increase. The reason behind this phenomenon is the development of viscous forces and resistance in the nanofluid was triggered by each additional number of φ, hence improves the heat transfer rate.
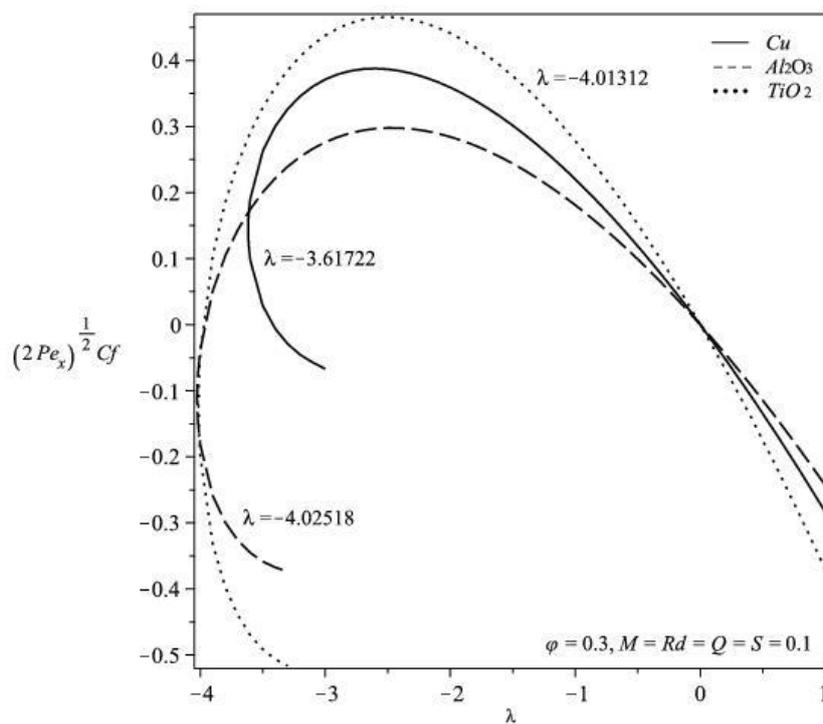

Fig. 2. Skin friction coefficients $\sqrt{2Pe_x}C_f$ against three types of nanoparticles

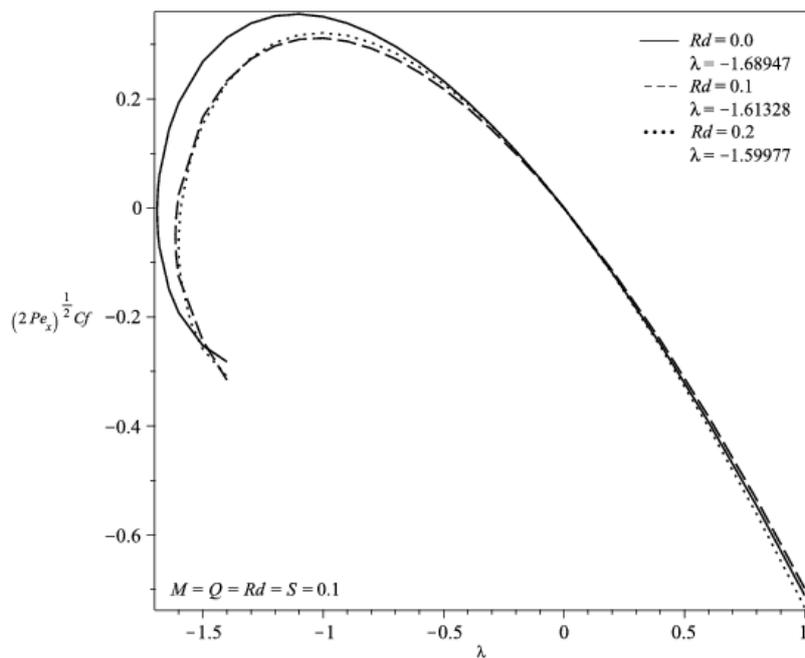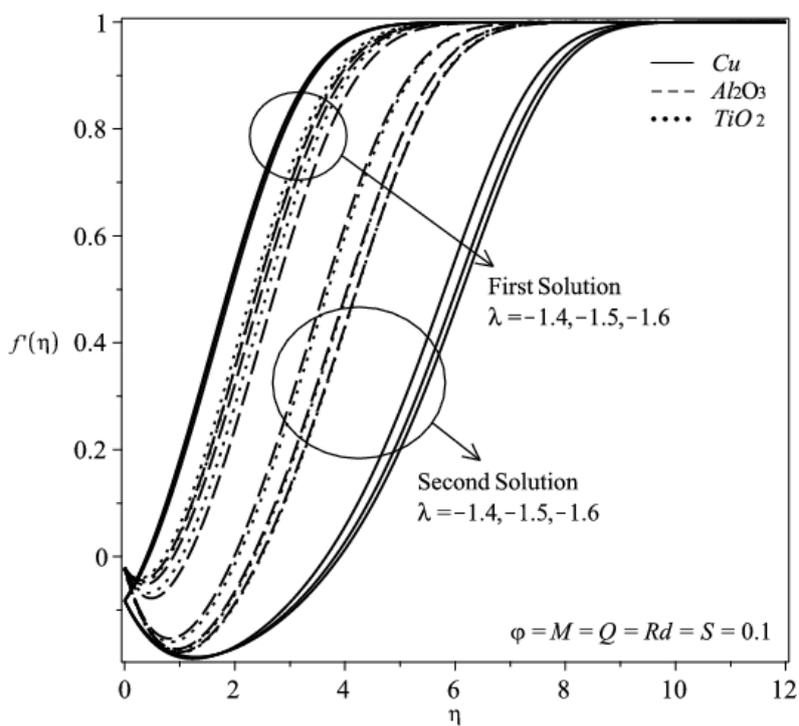**Fig. 3.** Skin friction coefficients $\sqrt{2Pe_x}C_f$ of Cu-water against Rd
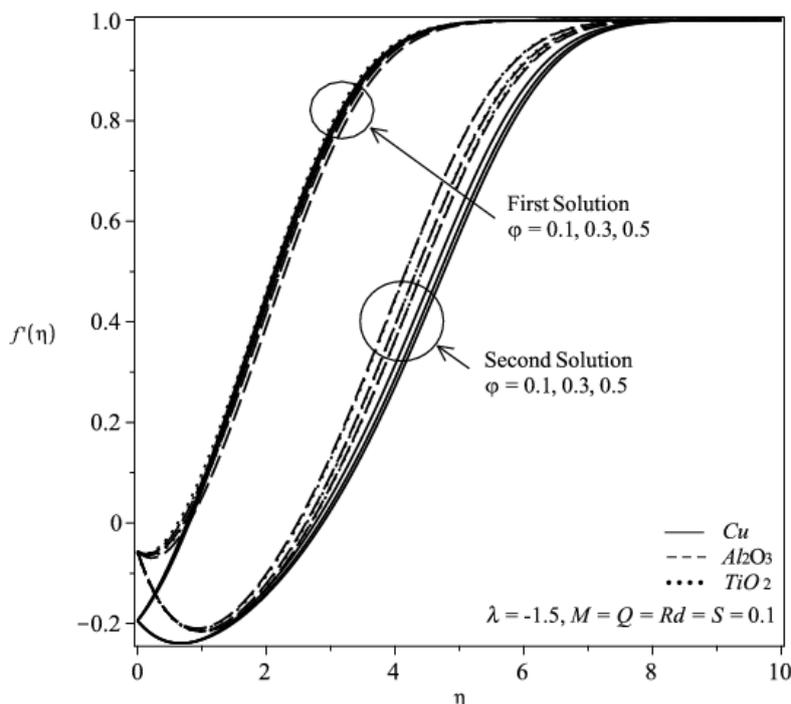

Fig. 4. Velocity profiles $f'(\eta)$ against λ

Fig. 5. Velocity profiles $f'(\eta)$ against φ

In our investigation into the effects of magnetic parameter *M* and radiation parameter *Rd* on velocity profiles $f'(\eta)$, we held other parameters at constant values. Two key figures, Figures 6 and 7, were used to depict the outcomes of these parameters on the function $f'(\eta)$. The influence of *M* on $f'(\eta)$ evidently shows that the boundary layer thickness behaved differently in the first and second solutions. This discrepancy indicates that *M* has a significant impact on the boundary layer, causing different velocity profiles depending on its value. On the other hand, Figure 7 demonstrates the effects of *Rd* and the first solution showed an increase in the boundary layer thickness, while the second solution exhibited a decrement. These findings suggest that *Rd* has a contrasting effect on the thickness of boundary layer compared to *M*. We then explored the effects of suction parameter *S* on $f'(\eta)$, as represented in Figure 8. The results were quite distinct: as the value of *S* increased, the boundary layer thickness increased in the first solution and decreased in the second solution. This implies that *S* has a profound impact on the motion of the nanoparticle, leading to changes in the velocity gradient at the surface. Moreover, suction was observed to trigger buoyancy forces, causing the heated fluid to move towards the wall. This phenomenon created a delay in velocity gradients, resulting in a mixed performance for both profiles. In essence, suction played a crucial role in accelerating the motion of nanoparticles.
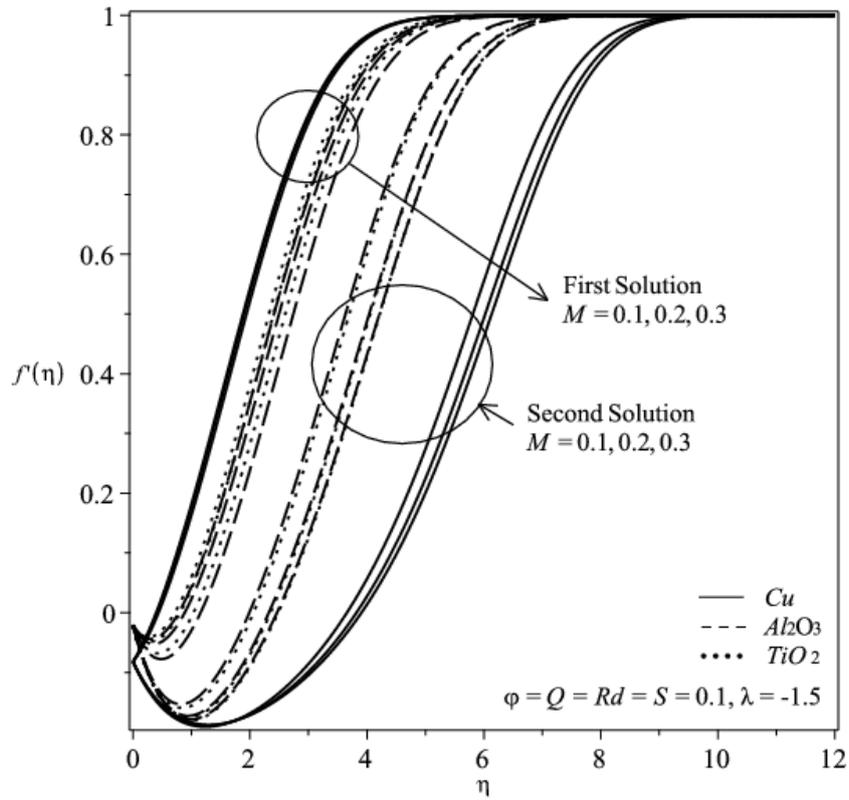
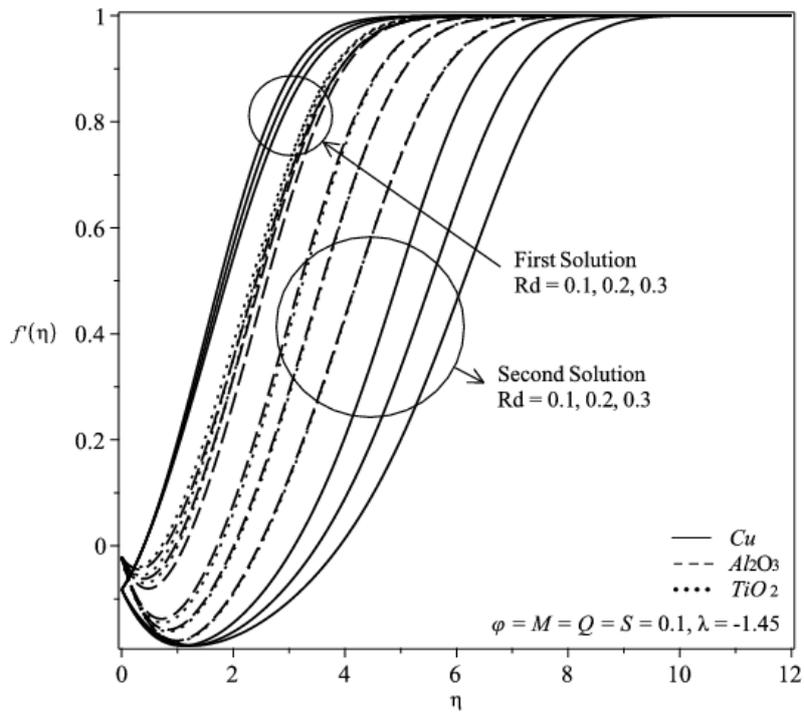**Fig. 6.** Velocity profiles $f'(\eta)$ against *M*

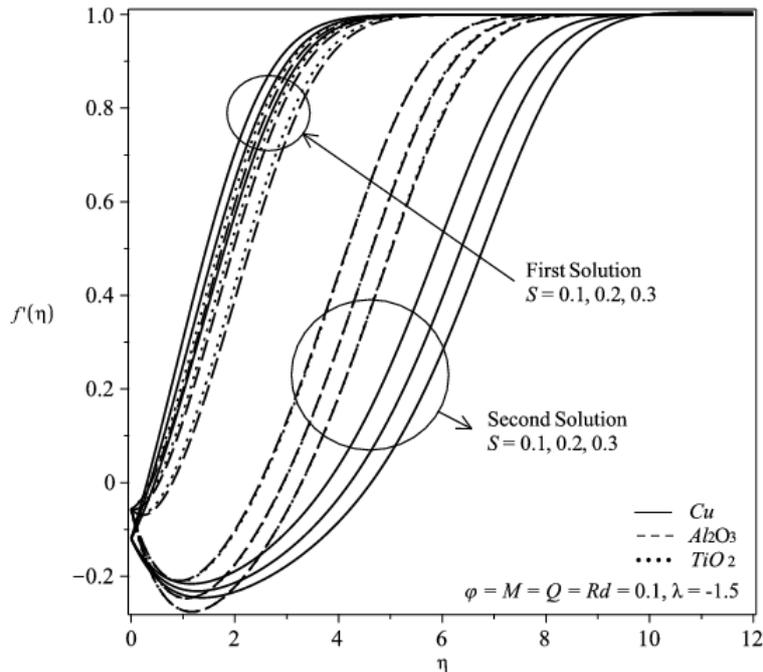**Fig. 7.** Velocity profiles $f'(\eta)$ against *Rd*

Fig. 8. Velocity profiles $f'(\eta)$ against S

4. Flow of Stability Analysis

4.1 Modelling of Stability Analysis

Stability analysis is conducted to distinguish the realizable physical solution between two branches of solutions associated with the mixed convection λ. To assess this condition, Weidman *et al.,* [46] and Merkin [47] proposed employing Eq. (2)-(4) in an unsteady state while keeping Eq. (1) constant. Prior to this, a new dimensionless time variable in the form of τ is introduced along with the similarity variables in Eq. (7)

$$\psi = \alpha_f \sqrt{Pe_x} f(\eta), \quad \theta(\eta) = \frac{T - T_\infty}{T_w - T_\infty}, \quad \eta = \sqrt{\frac{Pe_x}{2}} \frac{y}{x}, \quad \tau = \frac{U_\infty t}{x}. \tag{17}$$

where *t* represents time. In general cases, steady flow occurs when the flow parameters at any point in the fluid remain constant over time. However, unsteady flow can occur when the flow parameters, such as velocity, pressure, and density, are time-dependent and subjected to time-varying boundary conditions, oscillatory motions, or transient disturbances, see Bakar *et al.,* [48]. Thus, with the consideration of our unsteady mathematical models and Eq. (17), we have

$$\frac{\partial f}{\partial \eta} \left[\frac{1}{(1-\varphi)^{2.5}} - M \right] = \frac{1}{(1-\varphi)^{2.5}} + \left[(1-\varphi) + \frac{\varphi \rho_s \beta_s}{\rho_f \beta_f} \right] \lambda \theta - \frac{\partial^2 f}{\partial \eta \partial \tau}, \tag{18}$$

$$\frac{\partial^2 \theta}{\partial \eta^2} \left[\frac{k_{nf} / k_f}{(1-\varphi) + \frac{\varphi \rho_s C_{ps}}{\rho_f C_{pf}}} - \frac{4}{3} Rd \right] + f \frac{\partial \theta}{\partial \eta} + \frac{\rho_f}{\rho_{nf}} e^{-\eta} - \frac{\partial \theta}{\partial \tau} = 0, \tag{19}$$

It is worth mentioning that Eq. (18) and (19) can be combined to give a single equation as follows:

$$\frac{\partial^3 f}{\partial \eta^3} A - \frac{\partial^3 f}{\partial \eta^3}(1-\varphi)^{2.5} AM + A(1-\varphi)^{2.5} \frac{\partial^4 f}{\partial \eta^3 \partial \tau} - \frac{\partial^3 f}{\partial \eta^3} \frac{4}{3} Rd + \frac{4}{3} Rd (1-\varphi)^{2.5} M \frac{\partial^4 f}{\partial \eta^3 \partial \tau}$$
$$-\frac{4}{3} Rd (1-\varphi)^{2.5} \frac{\partial^4 f}{\partial \eta^3 \partial \tau} + f \frac{\partial^2 f}{\partial \eta^2} - f \frac{\partial^2 f}{\partial \eta^2}(1-\varphi)^{2.5} M + (1-\varphi)^{2.5} f \frac{\partial^3 f}{\partial \eta^2 \partial \tau} + \xi \lambda e^{-\eta} - B \frac{\partial \theta}{\partial \tau} = 0,$$

(20)

where $B = (1-\varphi)^{2.5}\left[(1-\varphi) + \frac{\varphi \rho_s \beta_s}{\rho_f \beta_f}\right]\lambda$, prior to the reduction of boundary conditions at

$$f(0,\tau) = S, \quad \frac{1}{(1-\varphi)^{2.5}} \frac{\partial f}{\partial \eta}(0,\tau) = \frac{1}{(1-\varphi)^{2.5}} + \left[(1-\varphi) + \frac{\varphi \rho_s \beta_s}{\rho_f \beta_f}\right]\lambda,$$
$$\frac{\partial f}{\partial \eta}(\eta,\tau) \to 1.$$

(21)

We test the solution stability of $f(\eta) = f_0(\eta)$ and $\theta(\eta) = \theta_0(\eta)$ to satisfy the boundary value problems by adopting [46] [47]

$$f(\eta,\tau) = f_0(\eta) + e^{-\gamma\tau} F(\eta,\tau), \quad \theta(\eta,\tau) = \theta_0(\eta) + e^{-\gamma\tau} G(\eta,\tau).$$

(22)

where γ is the growth or decay rate of disturbances and also known as the unknown eigenvalue. The solutions of eigenvalue give an infinite set of eigenvalues $\gamma_1 < \gamma_2 < ...$, signifying the growth or decay rate of a disturbance. Eigenvalues play a pivotal role in discerning the stability of a fixed point within a solution. If a solution's fixed point is stable and subjected to initial disturbances, it will eventually return to its original position and remain there [49] [50]. By substituting Eq. (22) into Eq. (20), we finally get:

$$F_0'''\left[A - (1-\varphi)^{2.5} AM - (1-\varphi)^{2.5} A\gamma - \frac{4}{3} Rd + \frac{4}{3} Rd (1-\varphi)^{2.5} M + \frac{4}{3} Rd (1-\varphi)^{2.5}\right] +$$
$$f_0 F_0''\left[1 - (1-\varphi)^{2.5} M - (1-\varphi)^{2.5} \gamma\right] + f_0'' F_0\left[1 - (1-\varphi)^{2.5} M\right] + B\gamma G_0' = 0,$$

(23)

along with the boundary conditions:

$$F_0(0) = 0, \quad F_0'(0) = 0,$$
$$F_0'(\eta) = 0 \text{ as } \eta \to \infty.$$

(24)

Later, Harris *et al.,* [51] emphasized that the condition of $F'(\eta) \to 0$ in Eq. (24) has been set at rest and replaced with the condition of $F''(\eta) = 1$ as $\eta \to \infty$.

4.2 Smallest Eigenvalue γ

Since there are dual solutions in certain range of parameters, we performed a stability analysis to identify which solution is stable between two solutions by finding the smallest eigenvalue γ. The values of eigenvalue as in Eq. (24) subjected to the boundary conditions in Eq. (25) were programmed numerically via bvp4c function in MATLAB. Table 3 shows the smallest eigenvalue γ for selected values of *Rd* while Table 4 listed the smallest eigenvalue γ for various values of φ. From these two tables, it is clearly seen that a series of positive amounts are observed in all first branch of solution, while the second solution is distinguished to be in a series of negative numbers as can be noticed in these two tables. Thus, from the definition of eigenvalue γ, a firm conclusion can be drawn as the first branch is stable and the second solution is unstable.

Table 3
Smallest eigenvalue γ against *Rd* and λ

Rd	λ	First Solution (Upper Branch)	Second Solution (Lower Branch)
	-1.4	0.5777	-1.8361
0.1	-1.5	0.5760	-1.5418
	-1.6	0.5742	-1.2135
	-1.4	0.6472	-1.8475
0.3	-1.5	0.3375	-1.5527
	-1.6	0.2253	-1.2138

Table 4
Smallest eigenvalue γ against φ and λ

φ	λ	First Solution (Upper Branch)	Second Solution (Lower Branch)
	-1.4	1.0829	-1.3229
0.2	-1.5	0.9991	-1.2249
	-1.6	0.9269	-1.1589
	-1.4	1.1319	-0.9862
0.3	-1.5	0.9908	-0.9767
	-1.6	0.8649	-0.9657

5. Conclusions

The study presents a numerical analysis and detailed discussion of the stability analysis on mixed convection boundary layer flow over a permeable surface embedded in a porous medium filled with a nanofluid, considering the presence of internal heat generation, MHD, and thermal radiation. We investigate the impact of various parameters, such as mixed convection parameter, nanoparticle volume fraction, magnetic parameter, radiation parameter, and suction parameter on the flow field. The results show the flow field is significantly influenced by these parameters, especially with the nanoparticle fraction. The increasing amount of percentage of each nanoparticle clearly exhibits a great improvement in both solutions of velocity profiles. For the three types of nanoparticles, it is observed that the boundary layer starts to separate faster for Al_2O_3 and TiO_2, which have similar characteristics, and followed by Cu. In cases where certain parameter ranges lead to dual solutions, a stability analysis was conducted to determine the stability of these solutions. It was found that the first solution initiates decay of disturbances, while the second solution initiates growth of disturbances. Consequently, it is concluded that the first solution is stable compared to the second solution.

Declaration Statement

The authors declare that there are no competing interests or personal affiliations that could influence the content of this work.

Acknowledgements

References

[[1]] Choi, S. US, and Jeffrey A. Eastman. *Enhancing thermal conductivity of fluids with nanoparticles*. No. ANL/MSD/CP-84938; CONF-951135-29. Argonne National Lab.(ANL), Argonne, IL (United States), 1995.

[2] Routbort, J. "Argonne national lab, michellin north america, st." *Gobain Corp* (2009).

[3] Wong, Kaufui V., and Omar De Leon. "Applications of nanofluids: current and future." *Advances in mechanical engineering* 2 (2010): 519659. https://doi.org/10.1155%2F2010%2F519659

[4] Hosseini, S. R., M. Sheikholeslami, M. Ghasemian, and D. D. Ganji. "Nanofluid heat transfer analysis in a microchannel heat sink (MCHS) under the effect of magnetic field by means of KKL model." *Powder Technology* 324 (2018): 36-47. https://doi.org/10.1016/j.powtec.2017.10.043

[5] Maleki, Hamid, Jalal Alsarraf, Abbas Moghanizadeh, Hassan Hajabdollahi, and Mohammad Reza Safaei. "Heat transfer and nanofluid flow over a porous plate with radiation and slip boundary conditions." *Journal of Central South University* 5, no. 26 (2019): 1099-1115. https://doi.org/10.1007/s11771-019-4074-y

[6] Du, Ruiqing, DanDan Jiang, Yong Wang, and Kwok Wei Shah. "An experimental investigation of CuO/water nanofluid heat transfer in geothermal heat exchanger." *Energy and Buildings* 227 (2020): 110402. https://doi.org/10.1016/j.enbuild.2020.110402

[7] Saffarian, Mohammad Reza, Mojtaba Moravej, and Mohammad Hossein Doranehgard. "Heat transfer enhancement in a flat plate solar collector with different flow path shapes using nanofluid." *Renewable Energy* 146 (2020): 2316-2329. https://doi.org/10.1016/j.renene.2019.08.081

[8] Kumar, Nishant, and Shriram S. Sonawane. "Experimental study of Fe2O3/water and Fe2O3/ethylene glycol nanofluid heat transfer enhancement in a shell and tube heat exchanger." *International Communications in Heat and Mass Transfer* 78 (2016): 277-284. https://doi.org/10.1016/j.icheatmasstransfer.2016.09.009

[9] Sheikholeslami, M., D. D. Ganji, and M. M. Rashidi. "Magnetic field effect on unsteady nanofluid flow and heat transfer using Buongiorno model." *Journal of Magnetism and Magnetic Materials* 416 (2016): 164-173. https://doi.org/10.1016/j.jmmm.2016.05.026

[10] Sheikholeslami, Mohsen, and K. J. A. M. Vajravelu. "Nanofluid flow and heat transfer in a cavity with variable magnetic field." *Applied Mathematics and Computation* 298 (2017): 272-282. https://doi.org/10.1016/j.icheatmasstransfer.2016.09.009

[11] Bahmani, Mohammad Hussein, Ghanbarali Sheikhzadeh, Majid Zarringhalam, Omid Ali Akbari, Abdullah AAA Alrashed, Gholamreza Ahmadi Sheikh Shabani, and Marjan Goodarzi. "Investigation of turbulent heat transfer and nanofluid flow in a double pipe heat exchanger." *Advanced Powder Technology* 29, no. 2 (2018): 273-282. https://doi.org/10.1016/j.apt.2017.11.013

[12] Nazari, Mohammad Alhuyi, Roghayeh Ghasempour, Mohammad Hossein Ahmadi, Gholamreza Heydarian, and Mohammad Behshad Shafii. "Experimental investigation of graphene oxide nanofluid on heat transfer enhancement of pulsating heat pipe." *International Communications in Heat and Mass Transfer* 91 (2018): 90-94. https://doi.org/10.1016/j.icheatmasstransfer.2017.12.006

[13] Jung, Sung Yong, and Hanwook Park. "Experimental investigation of heat transfer of Al2O3 nanofluid in a microchannel heat sink." *International Journal of Heat and Mass Transfer* 179 (2021): 121729. https://doi.org/10.1016/j.ijheatmasstransfer.2021.121729

[14] Barnoon, Pouya, and Davood Toghraie. "Numerical investigation of laminar flow and heat transfer of non-Newtonian nanofluid within a porous medium." *Powder Technology* 325 (2018): 78-91. https://doi.org/10.1016/j.powtec.2017.10.040

[15] Hassan, M., M. Marin, Abdullah Alsharif, and R. Ellahi. "Convective heat transfer flow of nanofluid in a porous medium over wavy surface." *Physics Letters A* 382, no. 38 (2018): 2749-2753. https://doi.org/10.1016/j.physleta.2018.06.026

[16] Ahmad, Sohail, Muhammad Ashraf, and Kashif Ali. "Bioconvection due to gyrotactic microbes in a nanofluid flow through a porous medium." *Heliyon* 6, no. 12 (2020). https://doi.org/10.1016/j.heliyon.2020.e05832

[17] Hayat, Tasawar, Farwa Haider, Ahmed Alsaedi, and Bashir Ahmad. "Unsteady flow of nanofluid through porous medium with variable characteristics." *International Communications in heat and mass transfer* 119 (2020): 104904. https://doi.org/10.1016/j.icheatmasstransfer.2020.104904

[18] Haq, Rizwan Ul, Ali Raza, Ebrahem A. Algehyne, and Iskander Tlili. "Dual nature study of convective heat transfer of nanofluid flow over a shrinking surface in a porous medium." *International Communications in Heat and Mass Transfer* 114 (2020): 104583. https://doi.org/10.1016/j.icheatmasstransfer.2020.104583

[19] Liu, Chunyan, Mingyang Pan, Liancun Zheng, and Ping Lin. "Effects of heterogeneous catalysis in porous media on nanofluid-based reactions." *International Communications in Heat and Mass Transfer* 110 (2020): 104434. https://doi.org/10.1016/j.icheatmasstransfer.2019.104434

[20] Nazari, Saeed, R. Ellahi, M. M. Sarafraz, Mohammad Reza Safaei, Ali Asgari, and Omid Ali Akbari. "Numerical study on mixed convection of a non-Newtonian nanofluid with porous media in a two lid-driven square cavity." *Journal of Thermal Analysis and Calorimetry* 140 (2020): 1121-1145. https://doi.org/10.1007/s10973-019-08841-1

[21] Shah, Zahir, M. Sheikholeslami, and Poom Kumam. "Simulation of entropy optimization and thermal behavior of nanofluid through the porous media." *International Communications in Heat and Mass Transfer* 120 (2021): 105039. https://doi.org/10.1016/j.icheatmasstransfer.2020.105039

[22] Siavashi, Majid, Mehdi Vahabzadeh Bozorg, and Mohammad Hesam Toosi. "A numerical analysis of the effects of nanofluid and porous media utilization on the performance of parabolic trough solar collectors." *Sustainable Energy Technologies and Assessments* 45 (2021): 101179. https://doi.org/10.1016/j.seta.2021.101179

[23] Habibishandiz, M., and M. Z. Saghir. "A critical review of heat transfer enhancement methods in the presence of porous media, nanofluids, and microorganisms." *Thermal Science and Engineering Progress* 30 (2022): 101267. https://doi.org/10.1016/j.seta.2021.101179

[24] Chamkha, Ali J., and A. M. Aly. "MHD free convection flow of a nanofluid past a vertical plate in the presence of heat generation or absorption effects." *Chemical Engineering Communications* 198, no. 3 (2010): 425-441. https://doi.org/10.1080/00986445.2010.520232

[25] Alsaedi, A., M. Awais, and T. Hayat. "Effects of heat generation/absorption on stagnation point flow of nanofluid over a surface with convective boundary conditions." *Communications in Nonlinear Science and Numerical Simulation* 17, no. 11 (2012): 4210-4223. https://doi.org/10.1016/j.cnsns.2012.03.008

[26] Mahmoudi, Ahmed, Imen Mejri, Mohamed Ammar Abbassi, and Ahmed Omri. "Analysis of the entropy generation in a nanofluid-filled cavity in the presence of magnetic field and uniform heat generation/absorption." *Journal of Molecular Liquids* 198 (2014): 63-77. https://doi.org/10.1016/j.molliq.2014.07.010

[27] Hosseini, S. R., M. Ghasemian, M. Sheikholeslami, Ahmad Shafee, and Zhixiong Li. "Entropy analysis of nanofluid convection in a heated porous microchannel under MHD field considering solid heat generation." *Powder technology* 344 (2019): 914-925. https://doi.org/10.1016/j.powtec.2018.12.078

[28] Mishra, Ashish, and Manoj Kumar. "Influence of viscous dissipation and heat generation/absorption on Ag-water nanofluid flow over a Riga plate with suction." *International Journal of Fluid Mechanics Research* 46, no. 2 (2019). https://doi.org/10.1615/interjfluidmechres.2018025291

[29] Akinshilo, Akinbowale T. "Thermal performance evaluation of MHD nanofluid transport through a rotating system undergoing uniform injection/suction with heat generation." *BioNanoScience* 9, no. 3 (2019): 740-748. https://doi.org/10.1007/s12668-019-00653-9

[30] O. Alzahrani, Ebraheem, Zahir Shah, Wajdi Alghamdi, and Malik Zaka Ullah. "Darcy–Forchheimer radiative flow of micropoler CNT nanofluid in rotating frame with convective heat generation/consumption." *Processes* 7, no. 10 (2019): 666. https://doi.org/10.3390/pr7100666

[31] Ali, Usman, M. Y. Malik, A. A. Alderremy, Shaban Aly, and Khalil Ur Rehman. "A generalized findings on thermal radiation and heat generation/absorption in nanofluid flow regime." *Physica A: Statistical Mechanics and its Applications* 553 (2020): 124026. https://doi.org/10.1016/j.physa.2019.124026

[32] Abdulkadhim, Ammar, Hameed K. Hamzah, Farooq Hassan Ali, Çağatay Yıldız, Azher M. Abed, Esam M. Abed, and Müslüm Arıcı. "Effect of heat generation and heat absorption on natural convection of Cu-water nanofluid in a wavy enclosure under magnetic field." *International Communications in Heat and Mass Transfer* 120 (2021): 105024. https://doi.org/10.1016/j.physa.2019.124026

[33] Ferdows, M., M. D. Shamshuddin, S. O. Salawu, and K. Zaimi. "Numerical simulation for the steady nanofluid boundary layer flow over a moving plate with suction and heat generation." *SN Applied Sciences* 3 (2021): 1-11. https://doi.org/10.1007/s42452-021-04224-0

[34] Elbashbeshy, Elsayed MA, Hamada Galal Asker, and Betty Nagy. "The effects of heat generation absorption on boundary layer flow of a nanofluid containing gyrotactic microorganisms over an inclined stretching cylinder." *Ain Shams Engineering Journal* 13, no. 5 (2022): 101690. https://doi.org/10.1016/j.asej.2022.101690

[35] Merkin, J. H. "On dual solutions occurring in mixed convection in a porous medium." *Journal of engineering Mathematics* 20, no. 2 (1986): 171-179. https://doi.org/10.1007/bf00042775

[36] Chamkha, Ali J. "Non-Darcy fully developed mixed convection in a porous medium channel with heat generation/absorption and hydromagnetic effects." *Numerical Heat Transfer, Part A Applications* 32, no. 6 (1997): 653-675. https://doi.org/10.1080/10407789708913911

[37] Yasin, Mohd Hafizi Mat, Norihan Md Arifin, Roslinda Nazar, Fudziah Ismail, and Ioan Pop. "Mixed convection boundary layer with internal heat generation in a porous medium filled with a nanofluid." *Advanced Science Letters* 13, no. 1 (2012): 833-835. https://doi.org/10.1166/asl.2012.3863

[38] Chamkha, Ali J., and Abdullatif Ben-Nakhi. "MHD mixed convection–radiation interaction along a permeable surface immersed in a porous medium in the presence of Soret and Dufour's effects." *Heat and Mass transfer* 44, no. 7 (2008): 845-856. https://doi.org/10.1007/s00231-007-0296-x

[39] Aydın, Orhan, and Ahmet Kaya. "Radiation effect on MHD mixed convection flow about a permeable vertical plate." *Heat and Mass Transfer* 45 (2008): 239-246. https://doi.org/10.1007/s00231-008-0428-y

[40] Shateyi, Stanford, Sandile Sydney Motsa, and Precious Sibanda. "The effects of thermal radiation, hall currents, soret, and dufour on MHD flow by mixed convection over a vertical surface in porous media." *Mathematical Problems in Engineering* 2010 (2010). https://doi.org/10.1155/2010/627475

[41] Makinde, O. D. "Heat and mass transfer by MHD mixed convection stagnation point flow toward a vertical plate embedded in a highly porous medium with radiation and internal heat generation." *Meccanica* 47 (2012): 1173-1184. https://doi.org/10.1007/s11012-011-9502-5

[42] Tiwari, Raj Kamal, and Manab Kumar Das. "Heat transfer augmentation in a two-sided lid-driven differentially heated square cavity utilizing nanofluids." *International Journal of heat and Mass transfer* 50, no. 9-10 (2007): 2002-2018. https://doi.org/10.1016/j.ijheatmasstransfer.2006.09.034

[43] Motsumi, T. G., and O. D. Makinde. "Effects of thermal radiation and viscous dissipation on boundary layer flow of nanofluids over a permeable moving flat plate." *Physica Scripta* 86, no. 4 (2012): 045003. https://doi.org/10.1088/0031-8949/86/04/045003

[44] Oztop, Hakan F., and Eiyad Abu-Nada. "Numerical study of natural convection in partially heated rectangular enclosures filled with nanofluids." *International journal of heat and fluid flow* 29, no. 5 (2008): 1326-1336. https://doi.org/10.1016/j.ijheatfluidflow.2008.04.009

[45] Ahmad, Syakila, and Ioan Pop. "Mixed convection boundary layer flow from a vertical flat plate embedded in a porous medium filled with nanofluids." *International Communications in Heat and Mass Transfer* 37, no. 8 (2010): 987-991. https://doi.org/10.1016/j.icheatmasstransfer.2010.06.004

[46] Weidman, P. D., D. G. Kubitschek, and A. M. J. Davis. "The effect of transpiration on self-similar boundary layer flow over moving surfaces." *International journal of engineering science* 44, no. 11-12 (2006): 730-737. https://doi.org/10.1016/j.ijengsci.2006.04.005

[47] Merkin, J. H. "On dual solutions occurring in mixed convection in a porous medium." *Journal of engineering Mathematics* 20, no. 2 (1986): 171-179. https://doi.org/10.1007/BF00042775

[48] Bakar, S. A., N. M. Arifin, N. Bachok, and F. M. Ali. "Hybrid Nanofluid Flow in a Porous Medium with Second-Order Velocity Slip, Suction and Heat Absorption." *Malaysian J. Math. Sci* 16 (2022): 257-272. https://doi.org/10.47836/mjms.16.2.06

[49] Abu Bakar, Shahirah, Norihan Md Arifin, Fadzilah Md Ali, Norfifah Bachok, Roslinda Nazar, and Ioan Pop. "A stability analysis on mixed convection boundary layer flow along a permeable vertical cylinder in a porous medium filled with a nanofluid and thermal radiation." *Applied Sciences* 8, no. 4 (2018): 483. https://doi.org/10.3390/app8040483

[50] Bakar, Shahirah Abu, Norihan Md Arifin, Roslinda Nazar, Fadzilah Md Ali, Norfifah Bachok, and Ioan Pop. "The effects of suction on forced convection boundary layer stagnation point slip flow in a darcy porous medium towards a shrinking sheet with presence of thermal radiation: A stability analysis." *Journal of Porous Media* 21, no. 7 (2018). https://doi.org/10.1615/JPorMedia.2018019722

[51] Harris, S. D., D. B. Ingham, and I. Pop. "Mixed convection boundary-layer flow near the stagnation point on a vertical surface in a porous medium: Brinkman model with slip." *Transport in Porous Media* 77 (2009): 267-285. https://doi.org/10.1007/s11242-008-9309-6